



An Experimental Analysis of Digital Elevation Models Generated with Lidar Data and UAV Photogrammetry

Nizar Polat¹  · Murat Uysal¹

Received: 12 October 2017 / Accepted: 8 February 2018 / Published online: 26 May 2018
© Indian Society of Remote Sensing 2018

Abstract

A digital elevation model (DEM) is a very important product that represents the topography digitally. It is an essential requirement of many engineering applications. From past to present, the methodology of DEM generation process is changed with respect to technology. Today, the laser scanner and aerial imagery are two widely used technologies to get DEM. Especially, the computer vision aided the use of unmanned aerial vehicles (UAV) opened new horizons in this regard. This study investigates the airborne LiDAR and UAV based DEM comparisons in terms of correlation and vertical accuracy. For this purpose four different LiDAR data are provided. Moreover, a photogrammetric flight is carried out with UAV and images of the study area are captured after field surveys. Then, five different DEMs are generated from five different point clouds. Finally, the statistical analyses are performed to calculate the correlations and accuracies of DEMs. According to the analysis, the UAV based models are as accurate as LiDAR based models along with some other advantages.

Keywords Photogrammetry · UAV · LiDAR · SFM · DEM

Introduction

Terrain or topography is one of the most necessary components in human life. For a long time, geography and cartography researchers have been studied on this issue in order to get a convenient definition and useful analysis of topography. This much effort is really necessary due to the high complexity of earth topography and it is impossible to get every detail. Thus the definition of topography involves an observation based scale of approximation (Xue-jun et al. 2007).

Today, thanks the developing technologies, a very large part of geographic and geomatic data is digitally obtained. Depending on this fact, the topography is produced in a digital format. In scientific literature, this phenomenon is called as a digital elevation model (DEM) which defines

the Z values of terrain surfaces digitally (Li et al. 2005; Guo'an et al. 2005; Xiong et al. 2014). In a further explanation, there are two kinds of DEM which are digital terrain model (DTM) and a digital surface model (DSM).

A DSM is a digital representation of the elevation related with the earth topography, including all natural and man-made objects. On the other hand a DTM looks like the DSM but in a way of the excluding all natural and man-made objects in order to define bare earth. A DTM can be obtained also by using several algorithms to remove objects from a DSM (Krauß and Pfeifer 1998; Vosselman 2000; Sithole and Vosselman 2004; Bandara et al. 2011; Krauß et al. 2011). A DEM can be produced by different kinds of data such as geodetic surveys, satellite imagery (optic or radar), aerial photographs (conventional or drone), and laser scanners (airborne or terrestrial) (Polat and Uysal 2015; Varlik et al. 2016). In last a few decades, the airborne Light Detection and Ranging (LiDAR) system has been a popular source of data to produce a DEM with the advantages of obtaining 3D points very effectively over an extensive study area in terms of both precision and time (Polat et al. 2015). LiDAR systems have very high economic weight due to the accuracy capability. Today it has

✉ Nizar Polat
nizarpolat@gmail.com

Murat Uysal
muysal@aku.edu.tr

¹ Geomatics Department, Faculty of Engineering, AKU, 03200 Afyon, Turkey

become one of the standard tools for topographic data acquisition as a result of the technological progress in laser scanners, Global Positioning System (GPS), inertial measurement unit (IMU) and aerial vehicles (Ullrich et al. 2008). Eventually, LiDAR data collecting for generating a DTM has become a widespread alternative to the traditional geodetic methods (Lohmann and Koch 1999).

On the other hand, the drones or unmanned aerial vehicle (UAV), has emerged as a low-cost alternative to the conventional photogrammetric system for an image capturing platform with high capability of spatio-temporal resolution to reach a variety of goals. It is also very useful for obtaining image based dense point cloud. In this way, it is possible to say that, UAV is an alternative data source for point cloud in the place of LiDAR. Some UAV based studies can be found in Eisenbeiss et al. (2005), Colomina et al. (2008), Remondino et al. (2011) and Uysal et al. (2013).

Although it is a clear fact that the UAV systems are a portable and flexible technology in collection of high resolution imagery, it still needs geomatic and computer vision approaches for DEM generation (Sona et al. 2014). According to some researchers, with the help of image processing algorithms, particularly the structure-from-motion (SfM), the UAV based photogrammetric applications including the DEM generation become easier (Harwin and Lucieer 2012; Westoby et al. 2012; Lucieer et al. 2014; Javernick et al. 2014; Prosdocimi et al. 2015). With all its advantages, today the UAV based DEM generation is becoming a serious rival to LiDAR. For more comprehensive information on DEM production with LiDAR and UAV, the Yilmaz and Uysal (2016), and Serifoglu Yilmaz and Gungor (2016) studies should be consulted. The main purpose of this study is to compare the LiDAR and UAV derived digital elevation models in terms of correlation and

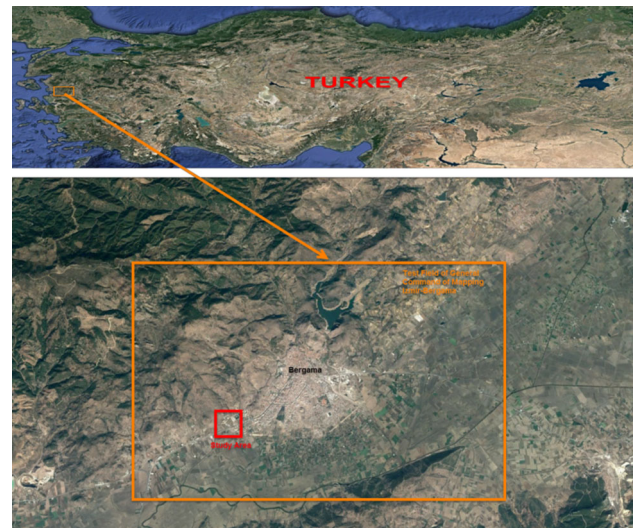


Fig. 1 The Google Earth image of the study area ($39^{\circ} 5'57.22''\text{N}$ – $27^{\circ} 8'59.77''\text{E}$)

accuracy. The performed analyses give information on the DEM generation in residential areas with LiDAR and UAV.

Study Area and Data Sets

The study area is a small part of the General Command of Mapping test field in Izmir–Pergamum with a coverage of 2.06 km^2 (Fig. 1).

The LiDAR data are collected by General Command of Mapping with Optech and Riegl laser scanners from 1200 to 2600 m altitude (Table 1). The altitude of the LiDAR system directly affects the data specifications such as density or intensity. In the meantime, scanning types also affect the density by means of duplicate points. These

Table 1 Optech and Riegl laser scanners basic specifications

Scanner	Scanning			
	Frequency	Angle	Type	Wavelength
Optech Pegasus HA-500	100–500 kHz	0° – 75°	Dual oscillating plane mirrors	Near infrared (1040–1060 nm)
Riegl LMS-Q1560	200–800 kHz	$58^{\circ}/60^{\circ}$	Rotating polygon mirror	Near infrared (1040–1060 nm)

Table 2 Point data specifications

	Raw points	Density (m^2)	Min Z (m)	Max Z (m)	Flight altitude (m)
UAV	30,461,747	8.76	57.16	126.86	100
R1200	10,736,475	6.07	60.31	126.91	1200
R2600	4,431,395	2.28	60.17	127.07	2600
O1200	9,474,475	4.91	60.61	126.92	1200
O2600	10,090,196	4.62	18.60	126.85	2600

Table 3 Calculated spatial resolutions (m)

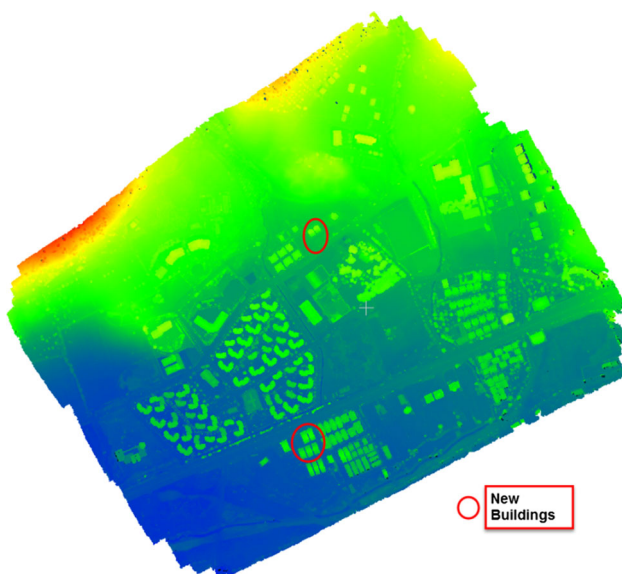
	Raw points	Ground points	Resolution (DSM)	Resolution (DTM)
UAV	30,461,747	26,138,351	0.26	0.28
R1200	10,736,475	9,308,739	0.44	0.47
R2600	4,431,395	3,764,116	0.68	0.51
O1200	9,474,475	8,064,957	0.47	0.50
O2600	10,090,196	8,670,808	0.45	0.49

differences allow us to get 4 different LiDAR data from a Riegl scanner (R1200 and R2600) and Optech scanner (O1200 and O2600). Furthermore, there is an image based dense point data which are generated from 420 images. The images are collected with DJI 3 Pro with an internal 12 MP camera. Additional specifications can be reached at Agisoft web site. Some information's about these 5 point data are in Table 2.

Methodology

Field Work

This section consists of field work, image processing, data filtering, and image interpolation. In field work, a flight plan is prepared and 7 ground control points (GCP) and 5 checked points (ChP) locations are determined. The GCP and ChP are marked on the ground and then surveyed with GPS before the flight. Preparing a flight plan is difficult due to the conditions such as obtaining flight permission, battery life time, and power lines. The flight performed as 14 columns with an altitude of 100 m from the initial ground.

**Fig. 2** New buildings on the study area**Table 4** Calculated correlation coefficients for DSMs

	UAV	R1200	R2600	O1200	O2600
UAV	1.000	0.961	0.963	0.953	0.948
R1200	0.961	1.000	0.980	0.979	0.973
R2600	0.963	0.980	1.000	0.972	0.971
O1200	0.953	0.979	0.972	1.000	0.978
O2600	0.948	0.974	0.971	0.978	1.000

The average ground sample distance is calculated as 7 cm. 420 collected images are selected for image processing.

Image Processing

The main objective of image processing is creating a dense point cloud. In scientific literature, the image based point cloud is obtained with structure from motion (SfM) approach. Despite the SFM operates under the same fundamental mathematical parameters of photogrammetry, this approach is developed in 1990s by computer vision and image processing community and is used as a feature-matching algorithm (Harris and Stephens 1988; Spetsakis and Aloimonos 1991; Boufama et al. 1993; Szeliski and Kang 1994). Briefly, it uses matched pixels of overlapping images to reach 3d structure of concerned object. Today, this method has reached a sufficient maturity and become commercial software such as Agisoft PhotoScan. At the end of the image processing, a dense 3D point cloud is obtained in an arbitrary coordinate system (Micheletti et al. 2015). The GCPs allow us to georeferencing of obtaining point cloud.

Point Cloud Filtering

As mentioned in the previous section, the DSM contains all object points of the study area but it needs only ground points in order to get DTM. In this purpose the point cloud is filtered by adaptive TIN filtering algorithm which is developed by Axelsson (2000). The algorithm is strong in handling surface discontinuities especially in urban areas (Polat and Uysal 2015). The algorithm operates by creating an initial triangular net to whole data and select seed

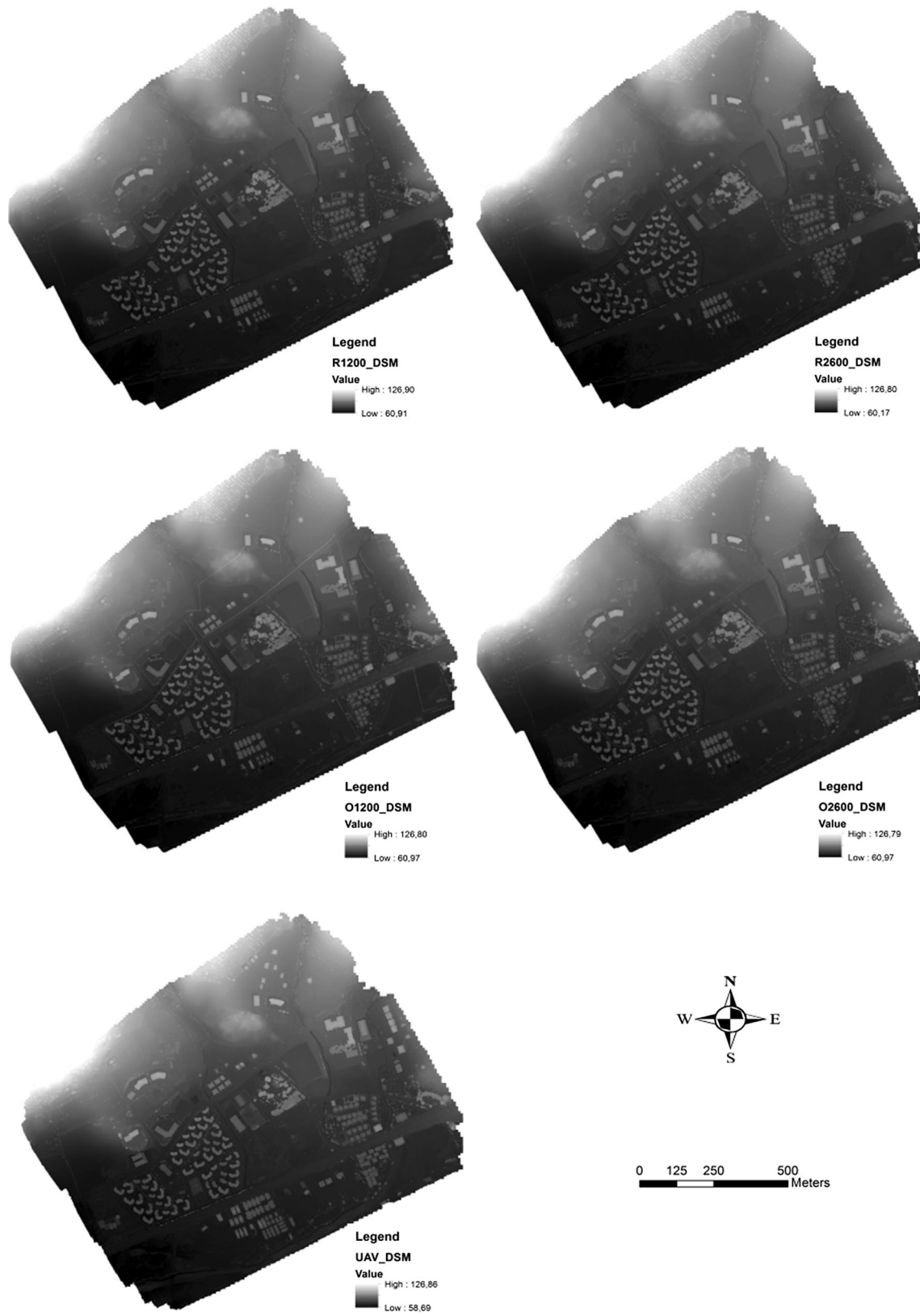


Fig. 3 Generated DSMs from LiDAR and UAV based point clouds

Table 5 Calculated correlation coefficients for DTMs

	UAV	R1200	R2600	O1200	O2600
UAV	1.000	0.964	0.959	0.970	0.972
R1200	0.964	1.000	0.983	0.984	0.978
R2600	0.959	0.983	1.000	0.978	0.977
O1200	0.970	0.984	0.978	1.000	0.983
O2600	0.972	0.978	0.977	0.983	1.000

points. Then by using a user defined threshold, all remaining points are compared and classified either ground or non-ground point. The threshold should be defined in consideration of the largest object in the data. Ultimately, the entire data set classifies as ground and non-ground.

Interpolation

In fact the generation of a digital elevation model from point data is an interpolation process which means fulfilling the every pixel to get a continuous raster data. There are lots of interpolation methods such as The inverse distance weighted, Kriging, and The Natural Neighbour. Based on previous experience, it is used the natural neighbour interpolation method in this study. This method is proposed by Sibson (1981). It is also called “area-stealing” interpolation. Mainly, the Voronoi and Delaunay charts are used for detecting the nearest point to input data. The height values of DEM are interpolated by means of input points. It can produce peaks, pits, ridges, or valleys that missing in the input samples. The generated digital surface is smooth everywhere and generally involves the all input points.

The interpolation process is directly related to the resolution. Depending on the point density, the ideal resolution of DEM alters. According to Hu (2003), the optimum spatial resolution of a digital model should be calculated with the following equation:

$$\text{Spatial Resolution} = \sqrt[2]{\frac{A}{n}} \quad (1)$$

where, n represents the number of ground points and A is the acreage of the study. This equality allows us to produce statistically the most appropriate spatial resolution.

Results and Analysis

In this section the DTMs and DSMs results are examined individually. In consideration of Table 2 and the Eq. 1, the DSMs are generated. But in the DTM resolution, the

calculation is performed with ground points that obtained filtering process. The calculated spatial resolutions are in Table 3.

Considering DEMs general usage, the resolution is taken as 0.5 m for all generated DSMs and DTMs. Before DEM analysis, the 4 different LiDAR point clouds are compared with UAV based point cloud by means of the iterative closest point algorithm. This algorithm is a direct cloud to cloud comparison approach. Between LiDAR data, the average maximum distance is calculated as 0.042 m which is expected. On the other hand, by using overlay analysis, the average maximum distance between LiDAR and UAV based point cloud is calculated as 23.78 m. This analysis also allows us to notice a few new buildings in the study area (Fig. 2).

The 5 different DSM are generated and a visually comparison performed. Except the new buildings, it is not possible to see any differences. So a raster based correlation is calculated (Table 4). Although there are changes between data, the correlations are still high.

The highest correlation coefficient between UAV and LiDAR is 0.963 and the highest correlation coefficient among LiDAR is 0.980. All generated high resolution DSMs are in Fig. 3.

As mentioned before, only ground points are used to generate DTM. It is impossible to perform a visual comparison between DTMs. So the raster based correlation is calculated same as done above for DSMs (Table 5).

The highest correlation coefficient between UAV and LiDAR is 0.972 and the highest correlation coefficient among LiDAR is 0.984. All generated DSMs are in Fig. 4.

Besides the correlation, the errors in Z values of DTMs are calculated. In this purpose, the Root Mean Squared Errors (RMSE) were calculated according to Eq. 2.

$$\text{RMSE} = \sqrt{\frac{\sum (Z_{dtm} - Z_{ref})^2}{n}} \quad (2)$$

where Z_{dtm} is the elevation value from the produced DTM, and Z_{ref} is the related reference elevation from check points. n is number of the check points. The RMSE allows us to detect how near an interpolated point appropriate to used data points. In other words, for comprehending how accurate the interpolation process managed to fill the empty pixels based on the ground points. So, in order to get accuracy of DTM, five check points are used to calculate the RMSE (Table 6).

According to Table 6, the UAV based DTM is as accurate as LiDAR DTM. Although the best RMSE is 11.1 cm for Optech 1200 data, still UAV DTM is a serious rival with an RMSE of 15.7 cm. Moreover, the RMSE of UAV DTM is smaller than other 2 LiDAR based DTM. In

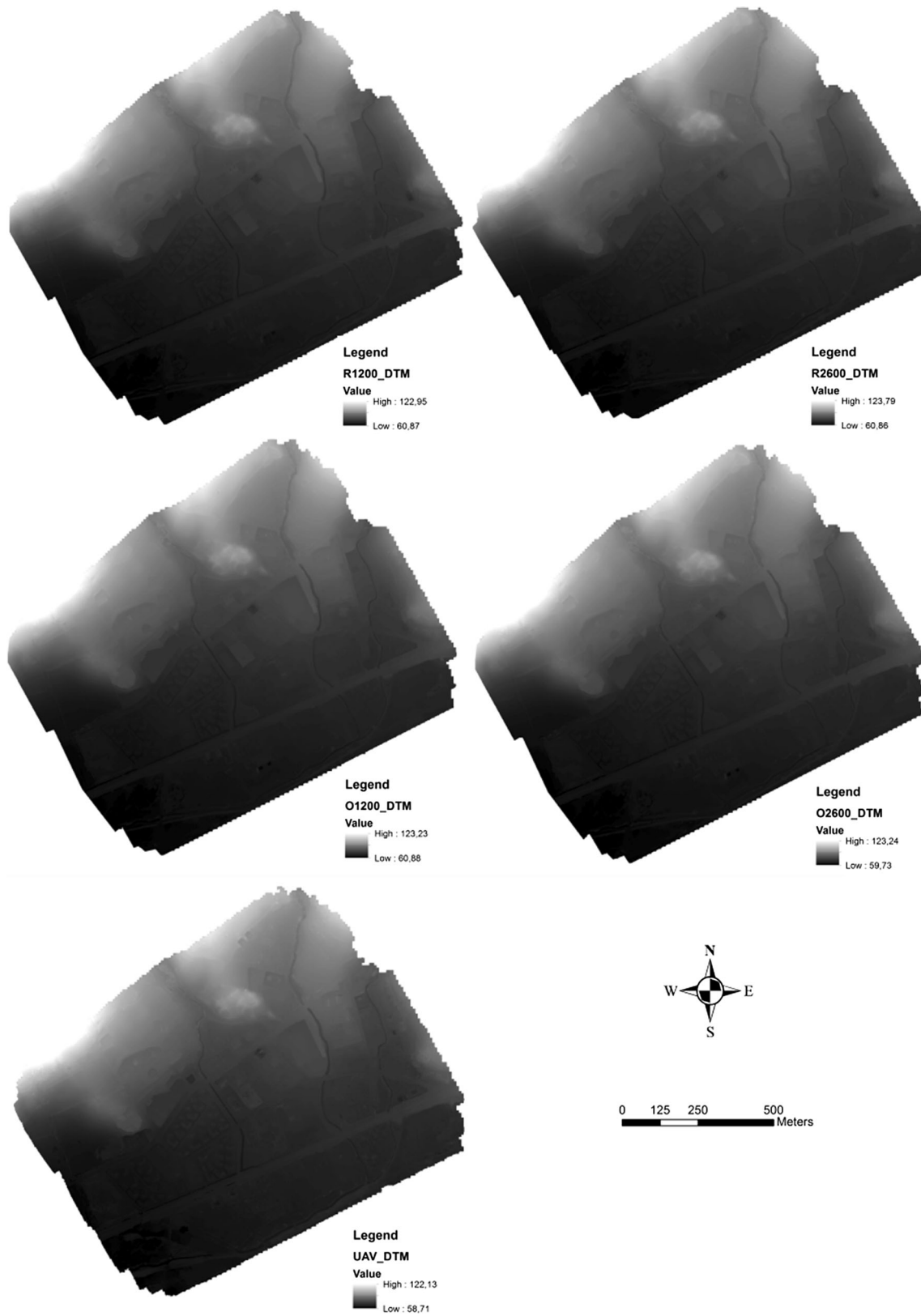


Fig. 4 Generated DTMs from LiDAR and UAV based point clouds

Table 6 Calculated root mean squared errors for DTMs (m)

	Reference	UAV	R1200	R2600	O1200	O2600
Point 1	68.375	68.16	68.501	68.495	68.55	68.54
Point 2	72.038	72.002	72.065	72.075	72.13	72.199
Point 3	67.054	67.085	67.049	67.044	67.091	67.062
Point 4	66.605	66.879	66.899	66.891	66.72	66.899
Point 5	65.812	65.825	65.962	65.874	65.9	65.899
	RMSE	0.157	0.158	0.143	0.111	0.172

Table 6, the bold value of 0.111 refers the minimum root mean square error among all DTMs. The maximum and minimum differences between LiDAR and UAV DTMs are 4.6 cm and 0.1 cm, respectively.

Conclusion

This study investigates the precision of digital elevation models (both DSM and DTM) which are generated from 4 different LiDAR data and UAV Photogrammetry. The main goal is to illustrate that the image based dense point cloud is as accurate as a LiDAR point cloud. According to the results, this goal is reached. The calculated root mean square errors clearly show that the UAV based DTM is second accurate one among all five DTMs with a 15.7 cm RMS error. So, in consideration of a relatively small size of the area, the UAV Photogrammetry can supply digital elevation models as accurate as LiDAR derived. Moreover, the UAV Photogrammetry is more economic, portable, and easy to use. It also provides urban change detection. But it should be noted that these results may give different results in different cameras, altitudes, software, and even lighting condition.

Acknowledgements This study is supported by Afyon Kocatepe University, Project Numbered 16.FEN.BIL.18.

References

- Axelsson, P. (2000). DEM generation from laser scanner data using adaptive TIN models. In *Proceedings of International Archives of Photogrammetry and Remote Sensing*, 33, 110–117.
- Bandara, K., Samarakoon, L., Shrestha, R. P., & Kamiya, Y. (2011). Automated generation of digital terrain model using point clouds of digital surface model in forest area. *Remote Sensing*, 3, 845–858. <https://doi.org/10.3390/rs3050845>.
- Boufama, B., Mohr, R., & Veillon, F. (1993). Euclidian constraints for uncalibrated reconstruction. In *Proceedings of computer vision conferences* (pp. 466–470). <https://doi.org/10.1109/iccv.1993.378179>.
- Colomina, I., Blázquez, M., Molina, P., Parés, M. E., & Wis, M. (2008). Towards a new paradigm for high-resolution low-cost

- photogrammetry and remote sensing. In *Proceedings of XXIst ISPRS congress: Technical commission I* (pp. 1201).
- Eisenbeiss, H., Lambers, K., Sauerbier, M., & Li, Z. (2005). Photogrammetric documentation of an archaeological site (Palpa, Peru) using an autonomous model helicopter. In *Proceedings of International CIPA Symposium* (pp. 238–243).
- Guo'an, T., Shanshan, G., Fayuan, L., & Jieyu, Z. (2005). Review of digital elevation model (DEM) based research on China Loess Plateau. *Journal of Mountain Science*, 2(3), 265–270.
- Harris, C., & Stephens, M. (1988). A combined corner and edge detector. In *Proceedings of the Alvey vision conference* (pp. 147–151).
- Harwin, S., & Lucieer, A. (2012). Assessing the accuracy of georeferenced point clouds produced via multi-view stereopsis from unmanned aerial vehicle (UAV) imagery. *Remote Sensing*, 4, 1573–1599. <https://doi.org/10.3390/rs4061573>.
- Hu, Y. (2003). *Automated extraction of digital terrain models, roads and buildings using airborne LiDAR data*. Dissertation, Department of Geomatic Engineering, University of Calgary.
- Javernick, L., Brasington, J., & Caruso, B. (2014). Modeling the topography of shallow braided rivers using structure-from-motion photogrammetry. *Geomorphology*, 213, 166–182. <https://doi.org/10.1016/j.geomorph.2014.01.006>.
- Krauß, T., Arefi, H., & Reinartz, P. (2011). Evaluation of selected methods for extracting digital terrain models from satellite born digital surface models in urban areas. In *Proceedings of the SMPR2011* (pp 1–7).
- Krauß, K., & Pfeifer, N. (1998). Determination of terrain models in wooded areas with airborne laser scanner data. *ISPRS Journal of Photogrammetry and Remote Sensing*, 53, 193–203. [https://doi.org/10.1016/S0924-2716\(98\)00009-4](https://doi.org/10.1016/S0924-2716(98)00009-4).
- Li, Z., Zhi, Q., & Gold, C. (2005). *Digital terrain modeling: Principles and methodology*. Boca Raton, FL: CRC Press.
- Lohmann, P., & Koch, A. (1999). Quality assessment of laser-scanner-data. In *Proceedings of the ISPRS workshop on sensing and mapping from space*, University of Hanover, Germany.
- Lucieer, A., Jong, S. M. D., & Turner, D. (2014). Mapping landslide displacements using structure from motion (SfM) and image correlation of multitemporal UAV photography. *Progress in Physical Geography*, 38, 97–116. <https://doi.org/10.1177/0309133313515293>.
- Micheletti, N., Chandler, J. H., & Lane, S. N. (2015). Structure from motion (SfM) photogrammetry. *Geomorphological Techniques*, 2, 1–12.
- Polat, N., & Uysal, M. (2015). Investigating performance of airborne LiDAR data filtering algorithms for DTM generation. *Measurement*, 63, 61–68.
- Polat, N., Uysal, M., & Toprak, A. S. (2015). An investigation of DEM generation process based on LiDAR data filtering, decimation, and interpolation methods for an urban area. *Measurement*, 75, 50–56.
- Prosdocimi, M., Calligaro, S., Sofia, G., Fontana, G. D., & Tarolli, P. (2015). Bank erosion in agricultural drainage networks: new challenges from structure-from-motion photogrammetry for post-event analysis. *Earth Surface Processes and Landforms*, 40, 1891–1906. <https://doi.org/10.1002/esp.3767>.
- Remondino, F., Barazzetti, L., Nex, F., Scaioni, M., & Sarazzi, D. (2011). UAV photogrammetry for mapping and 3d modeling—current status and future perspectives. In *Proceedings of the international archives of the photogrammetry, remote sensing and spatial information sciences*, Volume XXXVIII-1/C22 (pp 25–31).
- Serifoglu Yilmaz, C., & Gungor, O. (2016). Comparison of the performances of ground filtering algorithms and dtm generation from a UAV-based point cloud. *Geocarto International*, 32, 1–41. <https://doi.org/10.1080/10106049.2016.1265599>.

- Sibson, R. (1981). A brief description of natural neighbour interpolation. In V. Barnett (Ed.), *Interpreting multivariate data* (pp. 21–36). Chichester: Wiley.
- Sithole, G., & Vosselman, G. (2004). Experimental comparison of filter algorithms for bare-earth extraction from airborne laser scanning point clouds. *ISPRS Journal of Photogrammetry and Remote Sensing*, 59, 85–101. <https://doi.org/10.1016/j.isprsjprs.2004.05.004>.
- Sona, G., Pinto, L., Pagliari, D., Passoni, D., & Gini, R. (2014). Experimental analysis of different software packages for orientation and digital surface modelling from UAV images. *Earth Science Informatics*, 7, 97–107. <https://doi.org/10.1007/s12145-013-0142-2>.
- Spetsakis, M., & Aloimonos, J. Y. (1991). A multi-frame approach to visual motion perception. *International Journal of Computer Vision*, 6, 245–255.
- Szeliski, R., & Kang, S. B. (1994). Recovering 3d shape and motion from image streams using nonlinear least squares. *Journal of Visual Communication and Image Representation*, 5(1), 10–28.
- Ullrich, A., Studnicka, N., Hollaus, M., Briese, C., Wagner, W., Doneus, M., & Mücke, W. (2008). Improvements in DTM generation by using full-waveform airborne laser scanning data. In *Proceedings of the 7th annual conference and exposition "laser scanning and digital aerial photography. Today and tomorrow"*, 2008 Moscow, Russia.
- Uysal, M., Toprak, A. S., & Polat, N. (2013). Photo realistic 3d modeling with UAV: Gedik Ahmet Pasha mosque in Afyonkarahisar. In *Proceedings of the international CIPA symposium*, Volume XL-5/W2, Strasbourg, France.
- Varlik, A., Selvi, H. Z., Kalayci, I., Karauguz, G., & Ögütçü, S. (2016). Investigation of the compatibility of Fasillar and Eflatunpınar Hitite monuments with close-range photogrammetric technique. *Mediterranean Archaeology and Archaeometry*, 16(1), 249–256.
- Vosselman, G. (2000). Slope based filtering of laser altimetry data. In *Proceedings of the international archives of photogrammetry and remote sensing*, (Vol. XXXIII, pp. 935–942).
- Westoby, M. J., Brasington, J., Glasser, N. F., Hambrey, M. J., & Reynolds, J. M. (2012). 'Structure-from-Motion' photogrammetry: A low-cost, effective tool for geoscience applications. *Geomorphology*, 179, 300–314. <https://doi.org/10.1016/j.geomorph.2012.08.021>.
- Xiong, L. Y., Tang, G. A., Li, F. Y., Yuan, B. Y., & Lu, Z. C. (2014). Modeling the evolution of loess-covered landforms in the Loess Plateau of China using a DEM of underground bedrock surface. *Geomorphology*, 209, 18–26. <https://doi.org/10.1016/j.geomorph.2013.12.009>.
- Xue-jun, L., Hua-Xing, L., Zheng, R., & Zhi-feng, R. (2007). Scale issues in digital terrain analysis and terrain modeling. *Geographical Research*, 26(3), 433–442.
- Yılmaz, M., & Uysal, M. (2016). Comparison of data reduction algorithms for LiDAR-derived digital terrain model generalisation. *Area*, 48(4), 521–532. <https://doi.org/10.1111/area.12276>.